

Short Communication

Development of Tailor-Designed Gold-Platinum Nanoparticles Binary Catalysts for Efficient Formic Acid Electrooxidation

Islam M. Al-Akraa¹, Ahmad M. Mohammad^{2,3}, Mohamed S. El-Deab^{3,4}, Bahgat E. El-Anadoul^{3,*}

¹ Department of Basic Science, Faculty of Engineering, The British University in Egypt, Cairo 11837, Egypt

² Department of Chemical Engineering, Faculty of Engineering, The British University in Egypt, Cairo 11837, Egypt

³ Chemistry Department, Faculty of Science, Cairo University, Cairo 12613, Egypt

⁴ Department of Electronic Chemistry, Interdisciplinary Graduate School of Science and Engineering, Tokyo Institute of Technology, Midori-ku, 4259 Nagatsuta, Yokohama 226-8502, Japan

*E-mail: bahgat30@yahoo.com

Received: 19 March 2012 / Accepted: 7 April 2012 / Published: 1 May 2012

The modification of a glassy carbon (GC) electrode with platinum (PtNPs) and gold (AuNPs) nanoparticles is targeted to fabricate efficient anodes for the electrooxidation of formic acid (FA). A proper adjustment of the deposition sequence of PtNPs and AuNPs could eventually enhance the electrocatalytic activity of the electrode in such a way that suppresses the CO poisoning effect during FA oxidation. The highest catalytic activity is obtained at the Au/Pt/GC electrode (with PtNPs firstly deposited on the GC electrode followed by AuNPs). This superb enhancement is quantified by comparing the relative ratio of the direct vs. the indirect oxidation peaks at 0.3 and 0.65 V, respectively, at each electrode. The fundamental role of AuNPs (in Au/Pt/GC electrode) imparts immunity to the underlying PtNPs against CO poisoning by interrupting the contiguity of the Pt surface sites, thus, prevents the deterioration of the catalytic activity of the anode.

Keywords: Catalytic activity; Carbon monoxide; Fuel cells; Poisoning; Nanoparticles.

1. INTRODUCTION

Electrocatalysis at nanoparticles-based materials has been a subject of continuously growing interest, particularly for fuel cells applications [1]. Research in fuel cells is intensively growing with the global desire to obtain efficient, incessant, and green energy sources [2,3]. In this regard, the direct formic acid fuel cells (DFAFCs) have shown superiority over the traditional hydrogen and direct methanol fuel cells in providing electricity for portable electronic devices [4]. While hydrogen fuel

cells were limited by difficulties with hydrogen storage and transport, the direct methanol fuel cells (DMFCs) suffered from the inherent toxicity, and the slow oxidation kinetics of methanol as well as its high crossover through Nafion-based membranes [5]. On the other hand, FA exhibited a smaller crossover flux through Nafion membrane than methanol [6,7], allowing the use of high concentrated fuel solutions and thinner membranes in DFAFCs. This is highly desirable for the design of compact portable power systems. Furthermore, DFAFCs have a higher theoretical open-circuit potential (1.40 V) than that of hydrogen fuel cells (1.23 V) and DMFCs (1.21 V) [5,8]. Nevertheless, DFAFCs experience a severe drawback where the catalytic activity of the Pt anodes, on which the electrooxidation of FA proceeds, ceases with time. This results due to the adsorption of the poisoning CO intermediate resulting from the “*non-faradaic*” dissociation of FA. This ultimately deteriorates the overall performance of DFAFC.

The electrooxidation of FA on Pt adopts a dual path mechanism; the direct (at low potential domain - desired) and indirect (at high potential domain - undesired) pathways [9]. The direct pathway (I_p^d) involves the dehydrogenation of HCOOH molecule to CO₂. Whereas, the indirect pathway involves the adsorption of the dehydration product of HCOOH (i.e., CO) at low potential domain and its oxidation at a higher potential domain (I_p^{ind}). Therefore, it is the indirect pathway that generates CO, which intensely reduces the reaction rate at low anodic potentials.

In an attempt to overcome the CO poisoning, transition metal oxide nanostructures were deposited on Pt electrodes to mitigate such a poisoning effect of CO by providing oxygen species at relatively low anodic potentials thus facilitating the oxidation of CO [10]. Alternatively, interrupting the contiguity of the Pt surface atoms could help in this regard, as the indirect pathway of FA oxidation requires the existence of definite surface sites composed of at least three contiguous Pt atoms [11-13].

Herein, a simple procedure for the modification of GC electrode with the sequential deposition of Au and Pt nanoparticles is introduced. Minute amount of AuNPs could interrupt the contiguity of the Pt surface sites in such a way to impede the CO poisoning effect and to improve the catalytic efficiency towards the FA oxidation. We believe that the contiguity of the Pt surface sites is inherently influencing the catalytic activity of PtNPs modified electrodes towards FA oxidation. The influence of the AuNPs doping scheme on the catalytic efficiency is addressed.

2. EXPERIMENTAL

Typically-cleaned glassy carbon electrode (GC, $d = 3.0$ mm) was used as the working electrode. A spiral Pt wire and Ag/AgCl/KCl(sat) were used as the counter and reference electrodes, respectively. The electrodeposition of AuNPs on the bare GC and on PtNPs modified GC (Pt/GC) electrodes is carried out in 0.1 M H₂SO₄ containing 1.0 mM Na[AuCl₄] solution, and the potential was cycled between 0 and 1.1 V vs. Ag/AgCl/KCl(sat) at 100 mV s⁻¹ for 10 cycles. On the other hand, the electrodeposition of PtNPs on the bare GC and on AuNPs modified GC (Au/GC) electrodes was done in 0.2 M H₂SO₄ containing 1.0 mM H₂PtCl₆ solution via constant potential electrolysis at 1 V vs. Ag/AgCl/KCl(sat) for 300 s. All of the chemicals used in this investigation were of analytical grade and used without further purification.

The electrochemical measurements were performed at room temperature ($25\pm 1^\circ\text{C}$) in a conventional two-compartment three-electrode glass cell using an EG&G potentiostat (model 273A) operated with Echem 270 software. A field emission scanning electron microscope (FE-SEM, QUANTA FEG 250) coupled with an energy dispersive X-ray spectrometer (EDS) unit was employed to evaluate the electrode's morphology. The electrocatalytic activity of the modified electrodes toward formic acid oxidation was examined in a solution of 0.3 M FA at pH of 3.5 (the pH was adjusted by adding a proper amount of NaOH). Current densities were calculated on the basis of the real surface area of the working electrode.

3. RESULTS AND DISCUSSION

3.1. SEM Characterization

Several modifications for the GC electrode were employed for the sake of comparison. Figure 1(a and b) shows typical SEM images of the Pt/Au/GC and Au/Pt/GC modified electrodes respectively. For the Pt/Au/GC modified electrode (Fig. 1a), the AuNPs were directly electrodeposited on the GC electrode. Next, PtNPs were electrodeposited on the AuNPs modified electrodes.

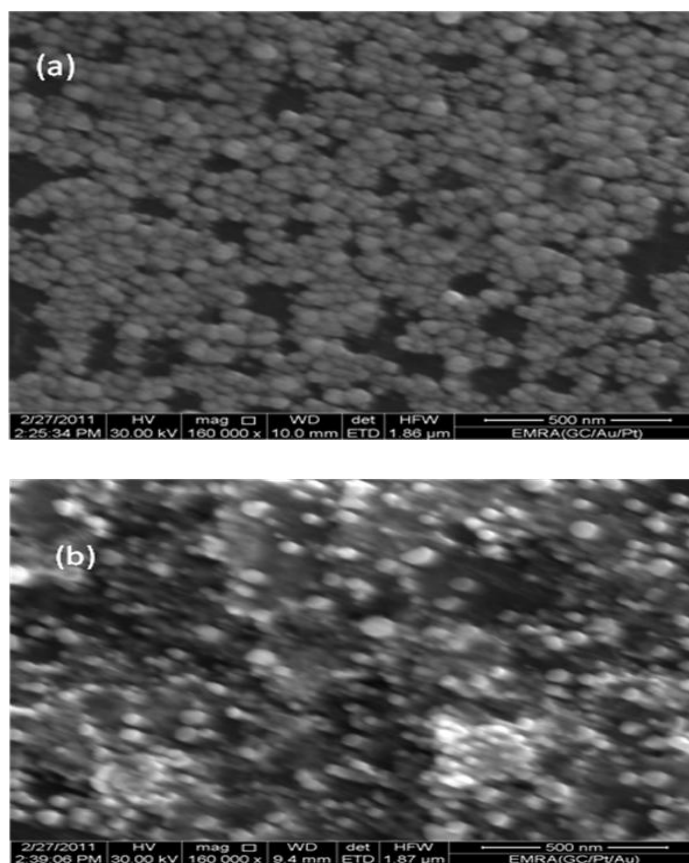


Figure 1. The FE-SEM micrograph of the (a) Pt/Au/GC and (b) Au/Pt/GC modified electrodes (magnification: 160,000 x)

Interestingly, as clearly shown in Figure 1a, AuNPs were completely covered with the PtNPs, resulting in what is called a core-shell structure. The average size of these structures was 45 nm.

On the other hand, in the Au/Pt/GC modified electrode (Fig. 1b), PtNPs were first electrodeposited on the GC electrode, and next AuNPs were deposited electrochemically. This procedure resulted in the deposition of Pt in the form of preferentially oriented nanorods (average diameter = 60 nm). Interestingly, the deposition of AuNPs on top of these nanowires resulted in the appearance of a decorated nanowire structure that homogeneously covered the entire surface of the GC electrode.

So far, the SEM characterization could not precisely distinguish the cases where PtNPs were deposited on AuNPs or directly on the GC electrode. Similarly, it could not inform whether AuNPs were deposited on PtNPs or directly on the GC electrode. This is actually a little bit difficult for SEM even when supported with a back scattered detector since Pt and Au have a comparable atomic weight. The electrochemical techniques will next be sought to evaluate the nature and sequence of these multistep depositions.

3.2. Electrochemical characterization

The electrochemical characterization methods are very powerful and sensitive to very low concentration even traces from the active ingredients, and can moreover, in certain circumstances, distinguish firmly between the different types of surface atoms as in our case of Au and Pt.

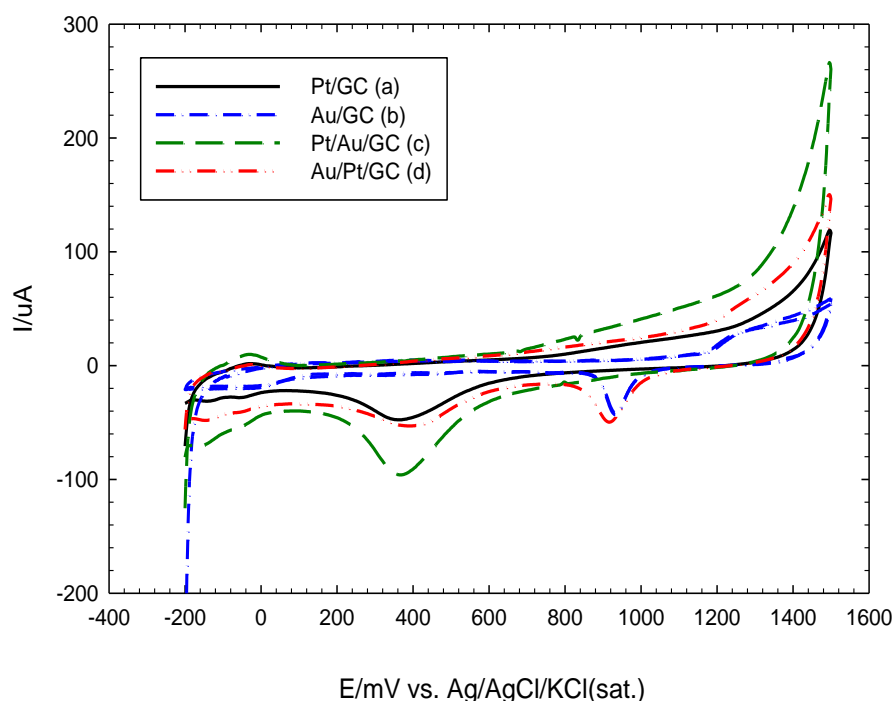


Figure 2. CVs obtained at (a) Pt/GC, (b) Au/GC, (c) Pt/Au/GC, and (d) Au/Pt/GC modified electrodes in 0.5 M H₂SO₄. Potential scan rate: 100 mV s⁻¹.

Figure 2 shows the typical Au and Pt characteristic CVs obtained at Pt/GC, Au/GC, Pt/Au/GC, and Au/Pt/GC modified electrodes in acidic conditions. In Figure 2a the characteristic behavior of a polycrystalline Pt electrode is clearly shown; the oxidation of Pt, which extends over a wide range of potential, is coupled with the reduction peak at 0.3–0.4 V vs. Ag/AgCl/KCl(sat). This couple corresponds to the solid-state surface redox transition (SSSRT) involving Pt/PtO. In addition, well-defined peaks for the hydrogen adsorption/desorption are shown in the potential range from 0.0 to –0.2 V vs. Ag/AgCl/KCl(sat). However, In Figure 2b, the gold oxide formation started at ca. 1.2 V vs. Ag/AgCl/KCl (sat.) and the oxide reduction peak appeared at ca. 0.9 V vs. Ag/AgCl/KCl (sat.).

Interestingly, Fig. 2c depicts that when PtNPs were deposited on the AuNPs-modified GC electrodes (Pt/Au/GC), the intensity of the Pt oxide reduction (at ca. 0.3–0.4 V) was increased if compared with that of the Pt/GC electrode (Fig. 2a). This can also be noticed in the Pt oxide formation and the hydrogen adsorption/desorption peaks of the Pt/Au/GC modified electrode. This behavior is likely related to a change in the exposed surface area available for the Pt deposition. In the Pt/Au/GC electrode, the deposition of AuNPs on the bare GC electrode could eventually increase the available surface area for the deposition of PtNPs. The SEM characterization in Fig. 1a, in addition, reflects the preference of the deposition of PtNPs on AuNPs rather than on GC surface. Hence, the increase in the PtNPs loading in the Pt/Au/GC modified electrode is expected.

On the other hand, when AuNPs were deposited on Pt/GC electrode (Fig. 2d), the exposed surface area of Pt changed a little (compare Figs. 2d and 2a). Very similar intensities of the reduction peak current of Pt oxide at 0.3–0.4 V can be observed. This indicates the preferential deposition of AuNPs on the GC rather than the PtNPs surfaces. This finding explores structural information that were not disclosed by SEM.

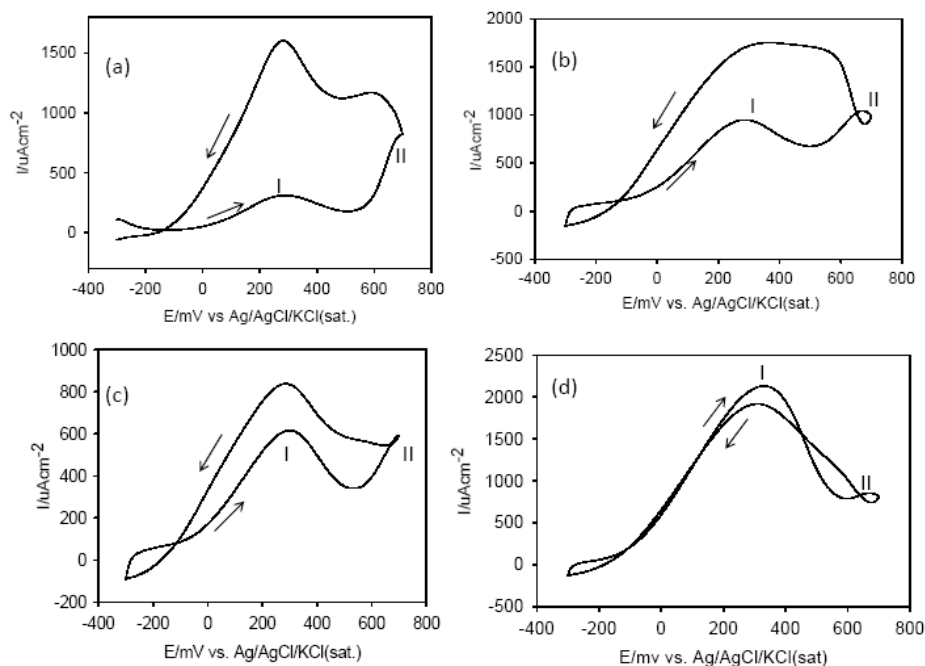


Figure 3. The CVs obtained at (a) bare Pt, (b) Pt/GC, (c) Pt/Au/GC, and (d) Au/Pt/GC electrodes in 0.3 M HCOOH (pH= 3.5). Potential scan rate: 200 mVs^{-1} .

A careful inspection for the Au oxide reduction peak at 0.9 V in the Au/GC, Pt/Au/GC and Au/Pt/GC electrodes (Figs. 2 b-d) reveals interesting points. At the Pt/Au/GC modified electrode (Fig. 3c), a complete absence of the Au oxide reduction peak is observed (note that the Pt oxide reduction peak appeared). This again strengthens our assumption that the AuNPs were completely coated by the PtNPs, and what is called a core-shell structure was developed. On the other hand, the appearance of the Au and Pt oxide reduction peaks at the Au/Pt/GC modified electrode (Fig. 3d) suggests the exposure of both of AuNPs and PtNPs at the surface and might support the preferential deposition of AuNPs on the bare GC rather on the PtNPs surface. This is reinforced after estimating the real surface area of AuNPs in the Au/GC and Au/Pt/GC modified electrodes which were approximately the same (0.08 cm^2).

3.3. Formic acid electro-oxidation

Figure 3 shows the CVs of the formic acid oxidation at the bare Pt, Pt/GC, Pt/Au/GC, and Au/Pt/GC electrodes in an aqueous solution of 0.3 M formic acid (pH = 3.5). At the bare Pt (Fig. 3a) and Pt/GC (Fig. 3b) electrodes, two peaks were observed in the forward scan, at ca. 0.3 V (peak I) and 0.65 V (peak II), respectively. The first peak at ca. 0.3 V (peak I) is assigned to the direct oxidation of HCOOH to CO_2 , while the second peak at ca. 0.65 V (peak II) is assigned to the oxidation of the poisonous CO_{ads} species to CO_2 . At low potential range, the Pt sites are partially poisoned by CO_{ads} from the dissociative adsorption step. The measured current then mainly comes from the FA oxidation on the unoccupied Pt sites through the dehydrogenation pathway. The peak current indicates the poisoning level of Pt surface by CO_{ads} . At high potential, the CO_{ads} is oxidized by Pt-OH species that starts to be formed at around 0.5 V during the forward scan, which releases most Pt sites for FA oxidation. In the backward scan (cathodic scan), while most of the poisonous intermediates have been oxidized at high potential, there were some of the poisonous intermediates still existed, so the indirect peak was still observed at the high potential region [14]. After the complete oxidation of the poisonous intermediates, the FA oxidation then can proceed on the clean Pt surface through the dehydrogenation pathway. Therefore, the current intensity which is proportional to the surface area, which was then refrained from CO poisoning, is expected to be high as depicted from Figures 3a and 3b.

We wish here to emphasize that the adsorption of CO on Pt surface requires the existence of three adjacent Pt sites (with a definite atomic spacing), and any interruption for this continuity may impede or prevent its adsorption [11]. In this regard, the modification of Pt-modified GC substrate with AuNPs in the Pt/Au/GC and Au/Pt/GC modified electrodes is intended to interrupt the Pt atoms contiguity required for CO adsorption. It worth mentioning that Au itself is a poor catalyst for the electro-oxidation of FA, where it cannot easily adsorb neither the reactant nor the intermediates [15]. The AuNPs-modified GC (Au/GC) electrode was therefore catalytically inactive towards the FA oxidation under the experimental conditions studied here (the results are not shown).

Two functions will next be employed to account on the degree of catalytic enhancement towards FA oxidation; one is the ratio of the current intensities of the direct peak (peak I) to the indirect peak (peak II) (I_p^d/I_p^{ind}), and the second is ratio of the current intensities of the forward direct

peak and the backward direct peak (I_p^d/I^b). At the Pt/Au/GC electrode, the ratio (I_p^d/I_p^{ind}) was comparable to that obtained at the Pt/GC electrode (ca. 2.3); however, the ratio (I_p^d/I^b) was increased from 0.5 to 0.7. This increase in (I_p^d/I^b) indicates improvement in catalytic activity of the Pt/Au/GC electrode towards FA oxidation, presumably, via lowering the CO adsorption and favoring the direct oxidation pathway.

Surprisingly, at the Au/Pt/GC electrode, the degree of enhancement towards the electro-oxidation of FA was outstanding, where a significant increase in the I_p^d/I_p^{ind} (ca. 25) and I_p^d/I^b (ca. 1.09) were obtained. This great enhancement in the catalytic activity of this electrode is likely related to the degree of interrupting the contiguity of the Pt sites necessary for CO adsorption [4]. At the Pt/Au/GC electrode, the PtNPs were deposited on the Au/GC electrode with a core-shell structure (Fig.2c), in which the AuNPs were entirely covered with the PtNPs. Hence, it was not surprising to observe the CO poisoning still influencing the electrode's catalytic activity (Fig. 3c). On the other hand, at Au/Pt/GC electrode, the AuNPs were deposited on the Pt/GC electrode in a decorated structure (Fig.2d) in which the AuNPs and PtNPs were both exposed at the surface. It is worth mentioning that the SEM and electrochemical investigations outlined above all support the preferential deposition of AuNPs on the bare GC surface rather than the PtNPs in the Au/Pt/GC electrode. This definitely cannot exclude the possibility of depositing minor amounts of AuNPs on the PtNPs (roughly estimated surface coverage was ~ 5%), and the slight variation in the real surface area of Pt before and after modifying the Pt/GC electrode with AuNPs ascertain that. The significant increase in the catalytic activity of the Au/Pt/GC electrode also recommends the deposition of minor amounts of AuNPs on the PtNPs; otherwise, there should be no change from the catalytic activity of the Pt/GC electrode.

We believe that the partial deposition of AuNPs on PtNPs (with surface coverage of ~ 5%) in the Au/Pt/GC electrode worked against the CO adsorption, which is necessary for the surface poisoning of the electrode. It, therefore, decreased the probability of surface poisoning and increased the catalytic activity towards the oxidation of formic acid (see Fig. 3d). It is actually interesting to achieve this level of reversibility and catalytic efficiency for the FA oxidation with a slight modification of the GC electrode. We will next work to optimize the loading level of both PtNPs and AuNPs in a way to achieve the highest catalytic activity towards the FA electrooxidation.

4. CONCLUSION

A slight modification for the GC electrode with PtNPs and AuNPs is intended for the electrocatalytic oxidation of FA. This modification targeted the surface modification of the contiguity of the Pt sites to resist the CO poisoning, which stands the main reason for the failure of the DFAFCs. Interestingly, the deposition sequence of PtNPs and AuNPs on the GC influenced to a great extent the electrode morphology and the catalytic efficiency. For example, at the Pt/Au/GC electrode, the PtNPs were deposited on the Au/GC electrode with a core-shell structure, while, at Au/Pt/GC electrode, the AuNPs were deposited on the Pt/GC electrode in a decorated structure. Alternatively, the highest I_p^d/I_p^{ind} ratio (ca. 25) was achieved on the Au/Pt/GC modified electrode.

References

1. A. Wieckowski, E.R. Savinova and C.G. Vayenas, *Catalysis and Electrocatalysis at Nanoparticle Surfaces*, first ed., Marcel Dekker, New York (2003).
2. A.M. Abdullah, T. Okajima, A.M. Mohammad, F. Kitamura and T. Ohsaka, *J. power sources*, 172 (2007) 209.
3. A.M. Abdullah, A.M. Mohammad, T. Okajima, F. Kitamura and T. Ohsaka, *J. Power Sources*, 190 (2009) 264.
4. S. Zhang, Y. Shao, G. Yin and Y. Lin, *J. Power Sources*, 195 (2010) 1103.
5. U.B. Demirci, *J. Power Sources*, 169 (2007) 239.
6. Y.W. Rhee, S.Y. Ha and R.I. Masel, *J. Power Sources*, 117 (2003) 35.
7. X. Wang, J.M. Hu and I.M. Hsing, *J. Electroanal. Chem.*, 562 (2004) 73.
8. X.W. Yu and P.G. Pickup, *J. Power Sources*, 182 (2008) 124.
9. A. Capon and R. Parsons, *J. Electroanal. Chem.*, 45 (1973) 205.
10. M.S. El-Deab, L.A. Kibler and D.M. Kolb, *Electrochem. Commun.*, 11 (2009) 776.
11. A. Cuesta, M.A. Escudero, B. Lanova and H. Baltruschat, *Langmuir*, 25 (2009) 6500.
12. M. Neurock, M. Janik and A. Wieckowski, *Faraday Disc.*, 140 (2009) 363.
13. I.M. Al-Akraa, A.M. Mohammad, M.S. El-Deab and B.E. El-Anadouli, *Chem. Lett.*, 40 (2011) 1374.
14. N. Kristian, Y. Yu, P. Gunawan, R. Xu, W. Deng, X. Liu and X. Wang, *Electrochim. Acta*, 54 (2009) 4916.
15. J.K. Lee, J. Lee, J. Han, T.H. Lim, Y.E. Sung and Y. Tak, *Electrochim. Acta*, 53 (2008) 3474